**Response to the Reviewers**

**Reviewer 1**

**Comment 1.1** — The manuscript by Luo et at. entitled "An explainable semi-supervised deep learning framework for mineral prospectivity mapping: DEEP-SEAM v1.0" (egusphere-2025-3283) describes a novel explainable semi-supervised deep learning framework for prospectivity mapping (MPM) of REE mineralisation in Northern Curnamona Province, South Australia. The newly developed DEEP-SEAM v1.0 tool and associated case study should be of interest to readers of EGUsphere and the broader community of (mathematical) geoscientists but the manuscript has some shortcomings that I believe will require major revisions before it can be considered for publication.

**Response:** Thank you for your thoughtful feedback on our manuscript. We greatly appreciate your comprehensive review and the helpful suggestions you provided in the attached PDF. We have carefully addressed each of your comments and made corresponding revisions to enhance the quality of our paper. **Note: As advised not to upload the revised manuscript during the response process, please refer to the attached document for more detailed information regarding the specific revisions made in response to your comments.**

**Comment 1.2** — The Introduction requires significant shortening by at least 33%. In its current format, it is too 'wordy' and presents a somewhat cumbersome read in that it contains too much technical detail, which would be better suited to the Materials and Methods section.

**Response:** Thank you for pointing this out. We agree and have relocated the technical details to the Materials and Methods section, making the Introduction more concise.

**Comment 1.3** — In my opinion, this section 'Geological Setting and REE Mineralisation' is the weakest part of your manuscript and one that requires significant strengthening. I understand that the focus of your study is on technology development and demonstrating the capabilities of the new newly developed DEEP-SEAM v1.0 tool. However, presenting a stronger more comprehensive targeting model would help to better position your manuscript and tool as well as generate greater impact and interest.

**Response:** We have substantially revised and expanded this section by incorporating additional details on the regional geological context. We added Lines 144-168: " Many of the Mount Painter region granites are extremely enriched in heat producing elements (U, Th, K), making this region notable for the significant heat generated by radiogenic decay of these elements. These High Heat Producing Granites (HHPG) serve as heat sources for hydrothermal circulation and have initiated convective sub-surface fluid migration, establishing a region of high geothermal gradient metamorphism (Kovacs, 2005; Neumann et al., 2000; Sandiford et al., 2002). The region has experienced a prolonged history of granitic intrusions and consequential localized radiogenic heating, spanning from the early Mesoproterozoic through the Delamerian Orogeny to the Late Palaeozoic. The Mesoproterozoic appears to have been particularly favourable for REE mineralisation, primarily attributed to: the generation of REE-enriched magmas and

relatively stable tectonic environments that enhanced the preservation potential of formed deposits. The close spatial association and genetic relationship between Mesoproterozoic stratigraphic units and known mineral occurrences further substantiate the critical significance of this geological period for regional REE mineralisation. This extended geological history has led to multiple phases and pulses of magmatic and hydrothermal activity. Mineralisation processes have been driven by two primary mechanisms: (1) initial stages involving the introduction of felsic magmatism, including direct fluid activity and heat originating from magmatic processes, and (2) subsequent stages driven by ongoing radiogenic heat generation from the uranium- and thorium-rich granites and the associated mobilisation of hydrothermal fluids (Hoatson et al., 2011). Throughout these processes, structural controls played a crucial role in ore formation, with fracture systems serving as primary conduits for mineralising fluids and magmas. These coupled magmatic and radiogenic heating processes have initiated extensive sodic, potassic, and chloritic alteration of the granites, locally transforming initial lithologies into gneisses and schists. The sustained hydrothermal activity has facilitated the formation of diverse mineral deposit types, including hydrothermal vein-type, breccia-hosted, and skarn-type deposits containing Au, Cu, U, Sn, and REEs, with REE mineralisation being particularly associated with both the initial felsic magmatic events and the long-term radiogenic heating effects of the HHPG."

Reference:

Kovacs, I.: Origin of the South Australian Heat Flow Anomaly. In: (Eds.) Amos Aikman, Katherine Lilly, Julien Celerier, Istvan Kovacs, and Giselle Estermann, An excursion guide to the Flinders Ranges, South Australia, Journal of the Virtual Explorer, Electronic Edition, ISSN 1441-8142, volume 20, paper 14, doi:10.3809/jvirtex.2005.00137, 2005.

Neumann, N., Sandiford, M., and Foden, J.: Regional geochemistry and continental heat flow: implications for the origin of the South Australian heat flow anomaly. Earth Planet. Sci. Lett. 183 (2000), 107-120, https://doi.org/10.1016/S0012-821X(00)00268-5, 2000.

Sandiford, M., McLaren, S. and Neumann, N.: Long-term thermal consequences of the redistribution of heat-producing elements associated with large-scale granitic complexes. J. metamorphic Geol., 20(1), 87-98. https://doi.org/10.1046/j.0263-4929.2001.00359.x, 2002.

Hoatson, D. M., Jaireth, S., and Miezitis, Y.: The major rare-earth-element deposits of Australia: geological setting, exploration, and resources, Geoscience Australia, 2011.

**Comment 1.4** — Restructure and expand your Table 1 to include additional information relating to host rocks (types and ages), host structures and ore controls, mineralisation styles, ore and gangue mineralogy, alteration types and assemblages, mineralisation ages, grade/tonnage information, etc.

**Response:** We have prepared an expanded Table 1 (please refer to the attached table) that incorporates the requested information.

Table 1: Overview of REE mineral occurrence characteristics (includes data from Drexel and Major, 1990; Edgecombe, 1998; Hore et al., 2020a; McPhee et al., 1982; Teale, 1995; Whitehead, 1976; Zivak, 2024)

| Location | Name | Commodity | Suggested mode of formation (mineralisation style) | Class code | Host Rock type | Host Rock age - Structure | Ore/gangue mineralogy | Alteration types and assemblages | REE Mineralisation ages | Grade/tonnage data |
|---|---|---|---|---|---|---|---|---|---|---|
| A (REE occurr | Yerila gneiss | Co, REE, Th, U | Metamorphosed and | Occurrence | gneiss | 1560 Ma | The Yerila Granite is generally | Fluorite crystallized early | unknown | n/a |

| Location | Name | Commodity | Suggested mode of formation (mineralisation style) | Class code | Host Rock type | Host Rock age - Structure | Ore/gangue mineralology | Alteration types and assemblages | REE Mineralisation ages | Grade/tonnage data |
|---|---|---|---|---|---|---|---|---|---|---|
| ence) | | | metasomatised sediments | | | | composed of large tabular K-feldspar phenocrysts and abundant biotite and contains allanite, fluorite, K-hastingsite, fluorapatite and titanate. Further accessories include uranothorites, uraninite, molybdenite, sphalerite, powellite, scheelite, bastnäsite-synchysite, chevkinite, pyrite and arsenopyrite. | in the sequence, as does some hastingsite (poikilitic texture) which is intergrown with biotite. However, hastingsite dominantly crystallized late in the sequence with most of the biotite (i.e. post-stress). Most accessories are included in the late-stage biotite. | | |
| B (REE occurrence) | Yerila East | REE | Metamorphosed and metasomatised sediments | Occurrence | As above | As above | As above | As above | As above | As above |
| C (Cu(-REE) occurrence) | Moolawatana | Cu, REE | Hydrothermal, Pneumatolytic or contact metamorphism | Occurrence | Within a narrow zone of Mesoproterozoic schists and quartzites lying between an augen granite variety and the Terrapinna Granite of the "Moolawatana Suite". | Host rocks are Mesoproterozoic in age (1580 Ma or older). The area is interpreted to lie on the western limb of a major southwest plunging regional antiformal structure. | The area contains a number of gossanous outcrops with surface evidence of copper mineralization in association with garnetiferous schists, quartz-garnet rocks and amphibolites. REE source is unknown, however, quartz sericite schists, | Within the sericite schists a fairly distinct Ce:Th ratio (approximately 1.7:1) is evident and is attributed to the presence of rare earth bearing allanite. | unknown | n/a |

| Location | Name | Commodity | Suggested mode of formation (mineralisation style) | Class code | Host Rock type | Host Rock age - Structure | Ore/gangue mineralology | Alteration types and assemblages | REE Mineralisation ages | Grade/tonnage data |
|---|---|---|---|---|---|---|---|---|---|---|
| | | | | | | | silvery in colour and locally garnetiferous, displays locally high radioactivity. These contain anomalous Ce and Th and this is thought to indicate the presence of a cerium bearing allanite. | | | |
| D (Cu(-REE) occurrence) | Gunsight Prospect | Cu, Co, REE, U | Pneumatolytic and skarn-type | Prospect | The Gunsight Cu, U deposit, although severely deformed, has an abundance of REE associated with pyrite hosted by quartz-chlorite-biotite (feldspar) tuffs. | Host rocks 1580 Ma. The primary ore body is hosted within sheared metasediments and metavolcanics and is juxtaposed against Box Bore Augen Gneiss to the east and west. The structural history of the Gunsight Prospect is one of polymetamorphism and multiple fold episodes. The Gunsight Prospect is thought to lie on the southeastern limb of a major antiform structure. Three fold phases are recognized. A number of major faults with associated shearing | The Gunsight Prospect mineralisation is in pyrite-rich units with copper sulphides - initially chalcopyrite. The sulphides have minor Co, As and Bi possibly incorporated in the pyrite. Rare-earth elements and uranium are highly concentrated into the pyritic units possibly in both monazite and apatite. Most of the rare- earth elements and uranium are in monazite although apatite has been reported with up to 11% total rare-earth elements. Locally, the rocks could contain up to 10% apatite and 10 - 35% monazite. | The Gunsight area contains several strato-tectonic units, separated by hydrothermally altered breccias. | Monazite grains from the Gunsight prospect dated around 460 Ma. | It contains (very) approximately 1 mill. Tonnes @ 0.5% Cu, 0.5% Co and 0.5kg U. |

| Location | Name | Commodity | Suggested mode of formation (mineralisation style) | Class code | Host Rock type | Host Rock age - Structure | Ore/gangue mineralology | Alteration types and assemblages | REE Mineralisation ages | Grade/tonnage data |
|---|---|---|---|---|---|---|---|---|---|---|
| | | | | | | and breccia zone development cut cross the Prospect. | Additionally rare earth bearing allanite and lanthanite is present. | | | |
| E (REE occurrence) | Four Mile Creek | REE | Metamorphosed sediments | Occurrence | Biotite schists, gneisses, granodiorites, quartzites. | Host rocks ~1580 Ma. | unknown | unknown | unknown | n/a |
| F (U(-REE) occurrence) | Armchair Prospect | U, Cu, REE, $U_3O_8$ | Hydrothermal | Deposit | In the general Mount Gee – Mount Painter area the basement rocks examined are composed mainly of quartz and microcline with minor sericite and mica, traces of apatite, altered ilmenite and zircon. Associated Devonian breccias -Cretaceous glacial sediments host the mineralisation. | Brecciated Mesoproterozoic and Late Cretaceous glacial sediments. | Monazite samples report elevated Ce and La. | Chlorite alteration associated with breccias. | unknown | n/a |
| G (U(-REE) occurrence) | Mount Gee East Deposit | U, REE | Hydrothermal | Occurrence | In the general Mount Gee – Mount Painter area the basement rocks examined are composed mainly of quartz and microcline with minor sericite and mica, traces of apatite, altered ilmenite and zircon. Associated Devonian breccias -Cretaceous glacial sediments host the | Brecciated Mesoproterozoic and Late Cretaceous glacial sediments. | Hematite (after magnetite) is associated with monazite and fergusonite. Uranium is associated with hematitic zones. REE are relatively abundant throughout the mineralised portions of the breccias, and in the Mount Gee Sinter. The combination of high cerium, | Magnetite alteration to ematite. | Monazite grains from the Mount Gee East Deposit dated around 360 Ma. | The resource estimate for the Mt. Gee uranium deposit remains at 31.3Kt* of contained U308 (2011). Values of 1% combined REE are found in hematitic breccia. |

| Location | Name | Commodity | Suggested mode of formation (mineralisation style) | Class code | Host Rock type | Host Rock age - Structure | Ore/gangue mineralology | Alteration types and assemblages | REE Mineralisation ages | Grade/tonnage data |
|---|---|---|---|---|---|---|---|---|---|---|
| | | | | | mineralisation. | | lanthanum, yttrium and phosphorus for these samples suggests that monazite is the source mineral. | | | |

Reference:

Drexel J.F. and Major R.B., 1990. Mount Painter uranium – rare earth deposits.    In F.E. Hughes (ed), Geology of the mineral deposits of Australia and Papua New Guinea. Australasian Institute of Mining and Metallurgy. Monograph Series 14:993–998.

Edgecombe D., 1998. Preliminary discussion on field trip to the Mt. Neil – Parabarana area, Period 3rd June to 11th June 1998. Goldstream Mining N.L. Department of Mines and Energy, South Australia Open File Envelope 9205, unpublished.

Hore, S. B., Hill, S. M., Reid, A., Wade, B., Alley, N. F., and Mason, D. R.: U–Pb geochronology reveals evidence of a Late Devonian hydrothermal event, and protracted hydrothermal–epithermal system, within the Mount Painter Inlier, northern Flinders Ranges, South Australia, Australian Journal of Earth Sciences, 67, 1009–1044, https://doi.org/10.1080/08120099.2020.1793383, 2020a.

McPhee K.A., Hodkinson I.P. and Mackie A.M., 1982. Report for Exploration Licence 871 (Gunsight) for 6 Month Period Ending 28 February, 1982. Department of Mines and Energy, South Australia. Open File Envelope 3536, unpublished.

Teale G.S., 1995. Exploration Licence 2173, "Arkaroola". Report on Geological Reconnaissance Work for Goldstream Mining N.L. Department of Mines and Energy, South Australia Open File Envelope 9205, unpublished.

Whitehead S., 1976. The Mineralology of some Mt. Painter Breccias.    AMDEL Petrological Report MP2714/76. unpublished.

Zivak D 2024. Rare Earth Element (REE) potential of the Curnamona Province, South Australia, Report Book 2024/00037. Department for Energy and Mining, South Australia, Adelaide.

**Comment 1.5** — The restructuring and expansion of Table 1 will go a long way to better demonstrate that the REE and U(-REE) and Cu(-REE) occurrences your work is based on form part of a coherent group of mineral deposit (i.e., part of a single mineral system). As a reader who is unfamiliar with these occurrences your manuscript does little to convince me of their similar origin. This is a critical issue as mixing mineral systems in MPM may give you garbage results.

**Response:**    We appreciate this important comment and have modified Table 1 as requested. However, we would like to respectfully clarify a fundamental aspect of our study design that addresses the reviewer's concern about mixing mineral systems. We do not propose that all REE, U(-REE), and Cu(-REE) occurrences originated from a single, unified mineral system. Rather, the study area represents a geologically complex terrain characterized by: (1) diverse sedimentary lithologies and granitic rocks; (2) multiple episodes of radiogenic heat-driven fluid circulation; (3) varying degrees of metamorphism and

structural deformation; and (4) complex fluid migration and recycling processes. Given this geological complexity, REE mineralization events cannot be attributed to a single metallogenic episode at a specific time. Importantly, our proposed MPM framework — particularly the deviation network method — is specifically designed to accommodate such multi-stage, multi-source metallogenic settings. Unlike traditional approaches that may indeed produce "garbage results" when different mineral systems are mixed, the deviation network method can effectively identify and discriminate different types of anomalous behaviors under partial constraints from known anomaly information (as explained in the methodology section). This approach does not conflate different mineral systems; rather, it systematically decouples and recognizes the related yet distinct signatures (remote sensing, geochemical, and geophysical) associated with multi-stage, multi-source mineralization processes. The delineation results of our prospective mineralization areas and their corresponding interpretations demonstrate the efficacy and validity of the proposed framework in handling geologically complex, multi-system terrains.

Regarding the data foundation: most of these 7 mineralization occurrences were targets obtained during mineral exploration in the 1970s. We have made considerable efforts to extract all available information from the limited historical exploration reports to provide the best foundation for understanding the relationship between mineralization characteristics and our input datasets. We acknowledge that such descriptions are not yet fully comprehensive, and we have expanded Table 1 to better present the available information. Further characterization of these occurrences remains an ongoing priority for future work.

**Comment 1.6** — Combine or link the improved Table 1 with Table 2 in a way that you clearly demonstrate which data map which expressions of the targeted mineral system.

**Response:** Table 2 is discussed with additional evidence demonstrating how our adopted datasets effectively support mineral prospectivity mapping. We added (1) Lines 201-205 Magnetic responses to REE mineralisation can be highly variable and depend on the nature of host rocks. White (2005) interprets the Yerila Granite (Table 1) in the study area not as a true granite (although parts of the protolith may have been deformed granite) but as a metasomatic allanite-rich rock, where the highest REE enrichment (Th, U, Zr, Y, and REEs) occurs in calcsilicate rocks that exhibit relatively distinct magnetic signatures compared to surrounding lithologies. (2) Lines 229-236:A compelling example of this relationship is demonstrated at REE Location D (Fig. 1), which represents a Cu-U-REE mineral system associated with hydrothermal fluid flow during the Ordovician (Zivak, 2024). The mineralisation is hosted within multiply deformed, pyrite-rich metasedimentary and metavolcanic rocks, where REEs and uranium are highly concentrated, predominantly in monazite and, to a lesser extent, in apatite (which locally contains up to 11% total REEs). Critically, both the radioactive elements and REEs were co-transported by hydrothermal fluids sourced from granitoid rocks along the eastern extremity of the Paralana Fault (Marshall, 1979). This genetic link between U-Th-K and REE enrichment provides a robust basis for using radiometric data as a proxy for REE prospectivity.. (3) Lines 247-257:Remote sensing is an important method for mineral prospecting, utilising hyperspectral and multispectral data to detect hydrothermally altered minerals with diagnostic spectral absorption characteristics (Pour and Hashim, 2011). Metasomatism plays a crucial geochemical role in the concentration of REEs, U, and Th, often producing diagnostic mineralogical assemblages detectable through remote sensing (Khoshnoodi et al., 2016). For example, Location A (Fig. 1), defined by the Yerila Granite, demonstrates intense metasomatic enrichment that can be captured by remote sensing data. The Yerila Granite (~1560 Ma, Moolawatana Suite) is geochemically unique, with extremely high REE contents and exceptional radioactivity, making it possibly the most radioactive granite in Australia (White, 2005; Sheard, 2009). This enrichment is attributed to metasomatic processes that produced

diagnostic REE-bearing minerals including allanite, monazite, yttrotitanite, and zircon, accompanied by K-feldspar alteration and fluorite mineralisation (White, 2005). These metasomatic assemblages and associated alteration minerals exhibit distinct spectral signatures in the visible-near infrared (VNIR) and shortwave infrared (SWIR) regions. (4) Lines 265- 274:For example, the high immediately to the west of REE Location G (Fig. 1), which is centred on Radium Ridge, demonstrates a clear relationship between topography and mineralisation. Radium Ridge is a prominent topographic feature extending approximately 3 km in an east-west direction, characterised by steep slopes on its southern flank and gentler gradients on the northern side (Sullivan et al., 1945). The steepest sections of the ridge result from differential weathering resistance of a silicified zone, which hosts small hydrothermal Fe-rich U and REE prospects along the ridge crest (Sullivan et al., 1945). This exemplifies how DEM data can capture the topographic expressions that result from structurally-controlled mineralisation and lithological contrasts caused by differential weathering and silicification processes, thereby serving as an indirect indicator of potential mineralised zones.

Reference:

White, A.J.: Granites and Uranium Mineralisation in the Mount Painter Complex Northern Flinders Ranges. PIRSA, Adelaide, Open File Envelope 12288, unpublished, 2005.

Zivak, D.: Rare Earth Element (REE) potential of the Curnamona Province, South Australia, Report Book 2024/00037. Department for Energy and Mining, South Australia, Adelaide, 2024.

Marshall, N.J.: Geochemical Exploration Studies in the Mt. Painter Province. Department of Mines and Energy, South Australia Open File Envelope 3536, unpublished, 1979.

Pour, A. B. and Hashim, M.: Identification of hydrothermal alteration minerals for exploring of porphyry copper deposit using ASTER data, SE Iran, Journal of Asian Earth Sciences, 42, 1309 – 1323, https://doi.org/10.1016/j.jseaes.2011.07.017, 2011.

Khoshnoodi, K., Yazdi, M., Behzadi, M., and Gannadi-Maragheh, M.: Using of ASTER, ETM+ and gamma spectrometry airborne data to find the relationship between the distribution of alkali metasomatism and REE mineralization in the Bafq area, Central Iran., Journal of Sciences, Islamic Republic of Iran, 27, 65 – 77, 2016.

Sheard, M.J.: Explanatory Notes for CALLABONNA 1:250000 Geological Map, sheet SH54-6. South Australia. Department of Primary Industries and Resources. Report Book, 2009/01, 2009.

Sullivan, C.J., Broadhurst, E., and Sprigg, R.C.: Reports on individual uranium occurrences. In Dickenson S.B. et al., eds, Report on investigation of uranium deposits at Mount Painter, South Australia [during the period] June 1944 to September 1945, Part III(3), Report Book 40/1. South Australia Department of Mines, Adelaide,. 124 – 168, 1945.

**Comment 1.7** — The study area is relatively small, in particular for an MPM study. Why did you not include the entire Mt Babbage and Mt Painter inliers, or at least the parts that are well exposed? That's not clear to me. Superimposing artificial, man-made boundaries on mineral systems should be avoided at all costs. At the very least, a clear explanation is required here as to the design of and rationale for the study area and its boundaries. Ideally, you should expand the study area to include the entire prospective tract. This should be easily possible given the great open-source data provided by the geological surveys of South Australia and New South Wales.

**Response:** Thank you for your thoughtful comment regarding the scope of the study area. We acknowledge that the current study area is relatively limited in size, particularly for an MPM study. This

was a deliberate design choice, driven primarily by the availability and quality of geochemical data, which are critical for accurately modeling REE mineralisation indicators. The constraint stems from the uneven distribution and sparsity of geochemical sampling points across the broader Mt Painter and Mt Babbage inliers. While open-source datasets offer excellent coverage for certain data types (e.g., geological maps and geophysical surveys), the geochemical datasets—essential for our DEEP-SEAM v1.0 tool's predictive modeling—present significant challenges. For instance:

Stream sediment and soil geochemical data provide limited useful elements relevant to REE prospectivity.

Rock geochemical datasets, while more comprehensive, suffer from partial element measurement gaps and highly irregular spatial distribution, with large tracts (please refer to the attached fig.1) lacking any sampling points altogether.

To mitigate these issues without introducing undue bias or inflating prediction uncertainties, we implemented a geospatial interpolation approach: for each grid point, we extracted geochemical samples within a 1.5 km radius, computed a weighted average using the inverse square of the distance as weights, and substituted the median elemental value where no nearby samples were available. This method allowed us to generate reliable geochemical layers for the core study area. However, extending this approach to the entire inliers would have required extrapolating over vast unsampled regions, potentially leading to artifacts, increased model uncertainty, and reduced interpretability of the results.

By confining the study area to regions with sufficient data density, we aimed to avoid superimposing unreliable predictions on the broader mineral system and to ensure the validity of our targeting model.
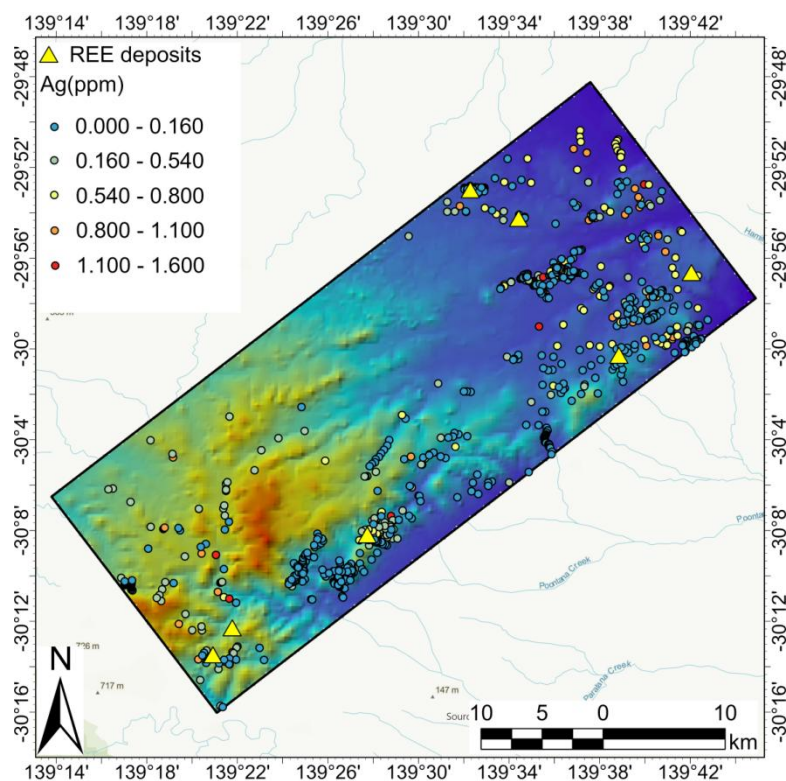
Figure 1. Spatial distribution of rock geochemical samples within an expanded study area.

**Comment 1.8** — Here you briefly refer to a "conceptual mineralisation model", which, however, is nowhere presented in the manuscript. This point links back to my above comments regarding the need for including a comprehensive targeting model that links mineralising processes to mappable ingredients of the

REE-U-Cu system and the datasets available for mapping the system footprints. See paper by McCuaig et al. (2010) for more information (https://www.sciencedirect.com/science/article/pii/S0169136810000612)

**Response:** In order to establish clear connections between mineralising processes → mineral system ingredients → mappable signatures → datasets, we have enhanced the "Geological Setting and REE Mineralisation" section with additional content, restructured Table 1, and strengthened the mineralisation-related justification for the datasets presented in Table 2.

**Comment 1.9** — How did you determine buffer zone sizes?

**Response:** Thank you for your questions about buffer zone determination and the negative sampling issues you raised in the PDF. The buffer zone sizes in our study were determined through systematic optimization involving iterative model training and performance evaluation. We tested multiple buffer sizes for each application and selected optimal values based on model performance metrics. This approach ensures both reproducibility and optimal model performance. As noted in your PDF comments, we deliberately selected negative samples from regions distal to known mineralized zones (typically >5 km away) to enhance model discrimination. This strategy follows established practice, as demonstrated by Zuo and Carranza (2011), who showed that proximal locations often exhibit similar multivariate spatial signatures to deposit sites, potentially creating biased training data and reducing model sensitivity. Our approach also follows the "near-mine exploration" principle, which recognizes that mineralization probability increases near known occurrences, thus justifying the exclusion of ambiguous near-deposit areas from negative sample pools.

Reference:

Zuo, R., & Carranza, E.J.M. (2011). Support vector machine: A tool for mapping mineral prospectivity. Computers & Geosciences, 37(12), 1967-1975.

**Comment 1.10** — Parts of the Discussion (highlighted in the attached commented PDF) deal with geology and methodology. These parts should be presented in the relevant Geology and Methods sections.

**Response:** Revised. These contents were moved to the appropriate positions.

**Comment 1.11** — Edge effects in Figure 10 (p. 29) must be discussed.

Response: We have conducted a comprehensive examination of the spatial statistical feature extraction process within buffer zones. While most input layers demonstrate normal statistical behavior, we acknowledge that a small number of layers exhibit pronounced standard deviation anomalies at the study area boundaries, manifesting as edge effects. This phenomenon primarily stems from statistical bias introduced by buffer truncation. We discuss this issue from three perspectives: data characteristics, model mechanisms, and prediction outcomes. From a data characteristics perspective, evidence layers exhibiting high-frequency spatial variations experience significant statistical bias when truncated at buffer edges due to insufficient sample points, resulting in amplified standard deviations (for instance, the AlOH_Group_Composition_Standard_Deviation layer shown in Fig. 10 in manuscript). Conversely, evidence layers with regional distribution characteristics maintain statistical consistency at boundaries, as their gradual variations are less susceptible to local truncation effects (such as the

AlOH_Group_Content_Standard_Deviation layer illustrated in the attached Fig. 2b). This disparity represents a classical manifestation of "edge effects" in spatial statistics, constrained by study area boundary conditions and fixed buffer radius settings. However, this issue is confined to a limited number of high-variability layers rather than being a systematic problem. Regarding model mechanisms, our framework employs the DevNet model based on multi-source exploration data for mineralization anomaly extraction. The model's core strengths lie in its multi-layer feature fusion strategy and anomaly learning mechanism, which enhance resistance to local noise including edge effects. DevNet establishes a robust "normality baseline" by learning the distribution patterns of extensive unlabeled samples and their differences from limited known mineralization samples in latent space. During training, the model is guided by prior mineralization information to learn anomaly patterns associated with mineralization rather than focusing on local anomalies and noise at boundaries, thereby effectively diluting the influence of edge effects in input data. In terms of prediction outcomes, both the prediction results and model interpretability analysis demonstrate that despite the significant presence of edge effects in certain evidence layers (such as AlOH_Group_Composition_Standard_Deviation) that play important roles in the model, the final mineral prospectivity map shows no apparent boundary artifacts such as edge-concentrated high values or anomalous gradients. This indirectly confirms that edge effects are progressively attenuated through multi-source data fusion and model learning processes, without compromising overall prediction accuracy and reliability. In summary, while edge effects objectively exist in a minority of input layers, their impact on final mineralization anomaly extraction reliability remains minimal due to the selective influence of data characteristics, DevNet's noise resistance mechanisms, and the stability of prediction results. We will consider extending buffer zones or implementing boundary correction algorithms for further optimization in future work.
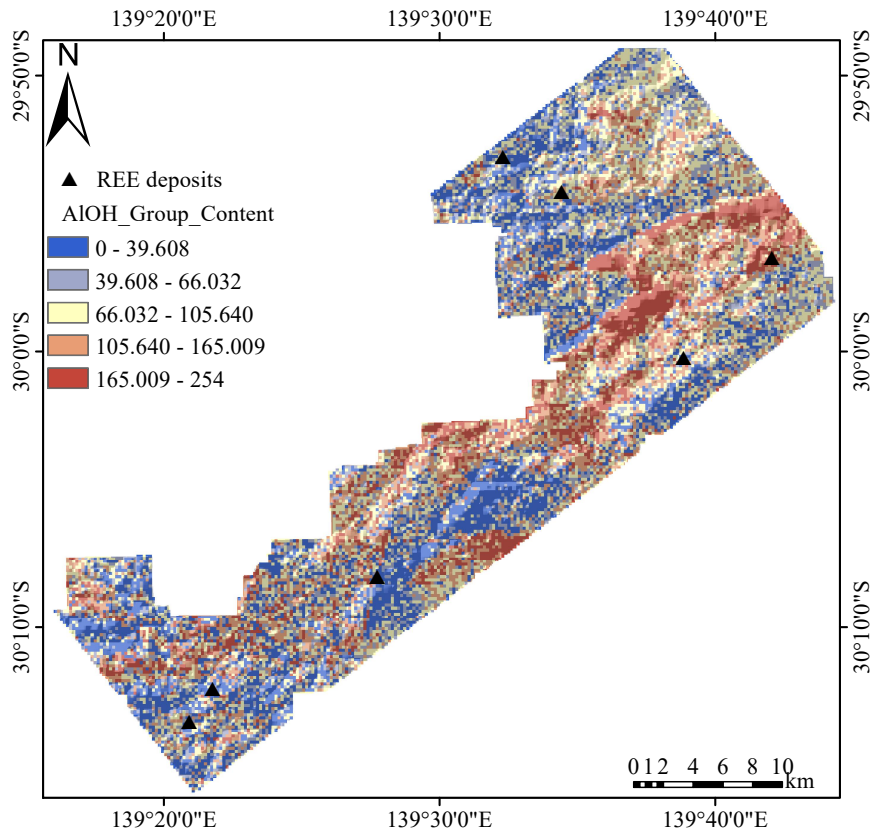
(a)
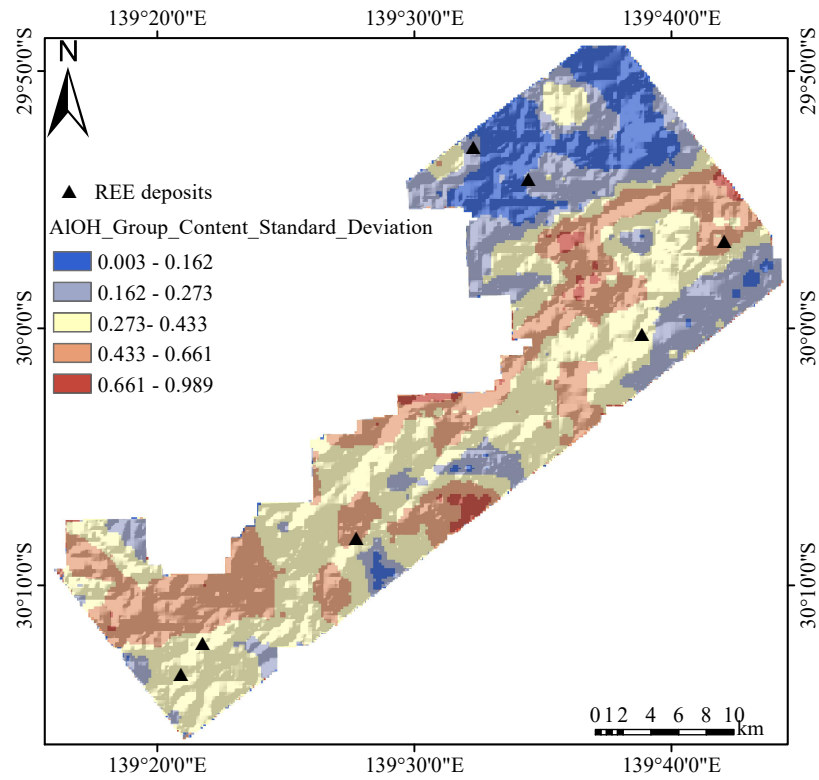
(b)

Figure2. ALOH Group Content: (a) original distribution; (b) standard deviation distribution

**Comment 1.12** 一 Additional minor comments are provided in the attached PDF.

**Response:** Thank you for your detailed review and the additional comments in the attached PDF. We have carefully addressed all suggested revisions in the revised manuscript. Regarding the additional questions outlined in the attachment, we will address each of them as follows:

1. Fig 1a - add rock type information and topgraphic contours.

Re: New figure as follows. However, adding topographic contours would make the figure cluttered, so we have overlaid a DEM to reflect topographic variations.
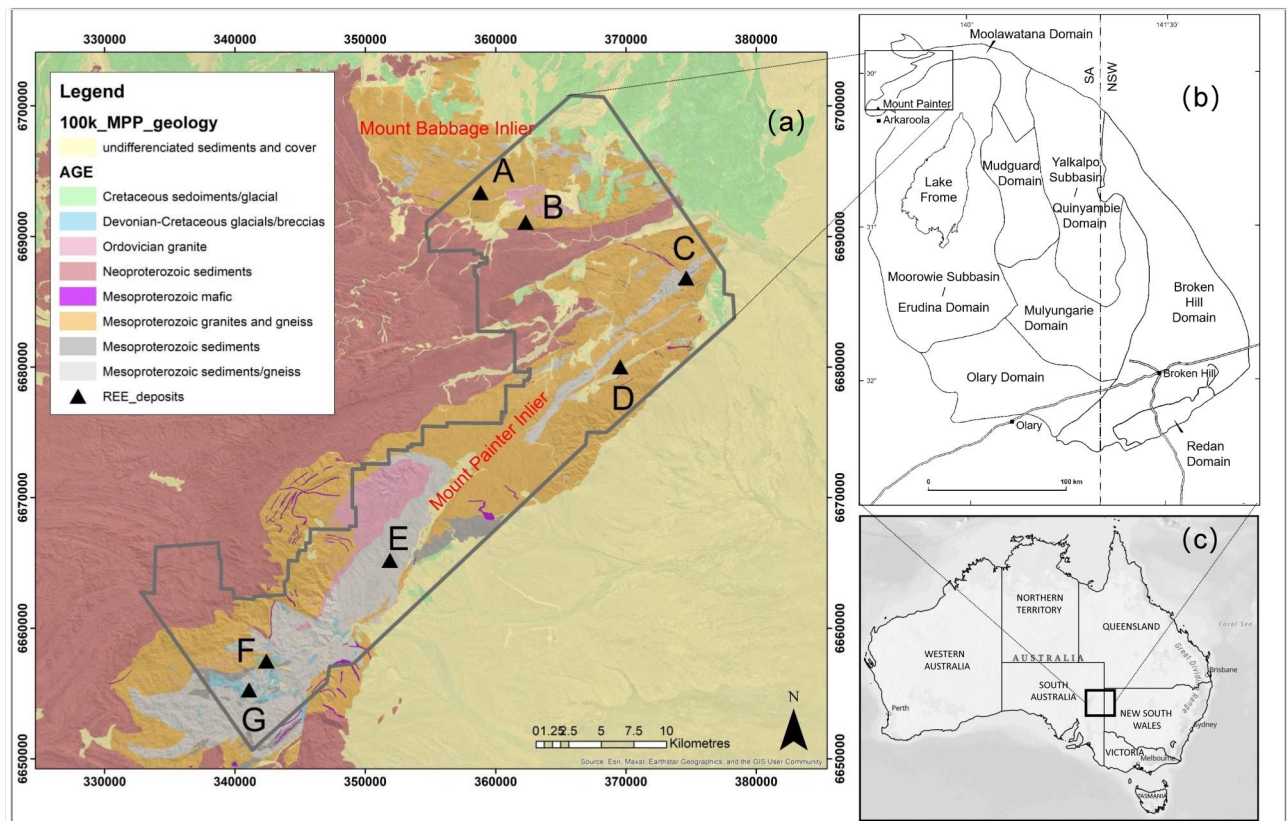
**Figure 3: (a) Simplified stratigraphic map and REE mineral deposits in the Mount Painter and Mount Babbage inliers of the north-western Curnamona Province; (b) Geographic location of the study area, after Jagodzinski and Fricke (2010); (c) Outline map of Australia with state borders.**

2. Use a 10 km scale bar. A 16 km scale bar is odd and not very useful.

Re: All figures are revised.

3. In Table1, "What is the difference betwen an occurrence and a prospect?"

Re:An outcrop or area with known REE minerals would be an occurrence, drilling or an extensive sampling program with analytical results could promote the known occurrence to a prospect especially if an ore estimate was suggested, the next step would be a resource...then mine.

4. How important are the REE you have assay data for (e.g., La and Sc) with regards to the occurrences in your study area? What concentrations of La, Sb etc. are recorded in these occurrences?

Re: The concentrations of REEs that can be collected from the deposits are all in our published dataset (https://doi.org/10.5281/zenodo.17098677; Luo et al., 2025).

5. In Table2, "Why is there no resolution (or mapping scale) provided here?"

Re : Revised.

6. In Figure3, "The REE pins are barely visible - enlarge here and in the inset figure below."

Re: Revised.

7. In Figure 5, "This is a pretty large bin. Why not add another one to better define areas of highest prospectivity? Ideally 75th percentile and up."

Re: In practice, the model outputs anomaly scores over a broad range, and we normalize these scores to the interval [0,1]. Then, we employed the Geometrical Interval classification specifically to address the strong right-skewed distribution of our dataset. Unlike quantile methods (e.g., percentiles), which force equal data counts per class, Geometrical Interval adapts to data density—creating narrower bins for the abundant low values and wider bins for the sparse high values. Consequently, the wide numerical range

of the highest class (0.3618 – 1.0) is intentional and geologically meaningful. It captures the 'long tail' of the distribution, representing a very small fraction of the study area (<8%). This effectively isolates the rare, top-tier targets. Subdividing this class further would arbitrarily fragment these significant outliers and potentially obscure the distinction between true high-prospectivity zones and background values.

8.  In Figure 7- 10, "(1) Use the same feature terminology as introduced in Table 2!; (2) Worthwhile adding an extra sentence to explain how this graph works using one of the fetures as an example"

Re: Revised. For example,
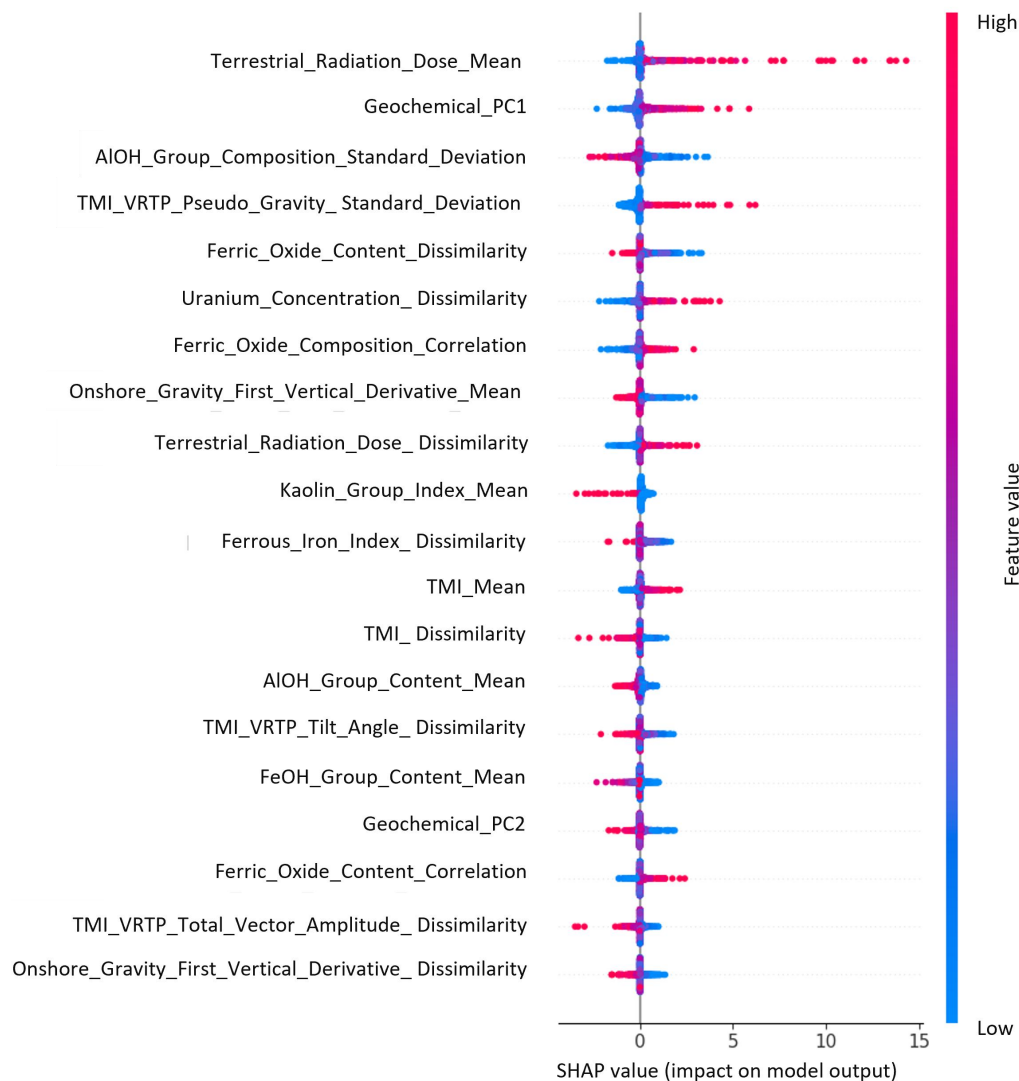
Figure 7: SHAP summary scatter plot illustrating the association between individual feature values and their corresponding predicted probability scores. Each dot represents a sample, with color indicating the feature value (red = high, blue = low) and horizontal position showing the SHAP value (positive = increases predicted prospectivity, negative = decreases prospectivity). For example, Terrestrial_Radiation_Dose_Mean, the most influential feature, shows that samples with high values (red dots) predominantly cluster on the positive side of the x-axis, while those with low values (blue dots) appear on the negative side. This pattern indicates that higher Terrestrial_Radiation_Dose_Mean values positively contribute to elevated mineralisation anomaly scores predicted by the model.